International Journal of
INTELLIGENT SYSTEMS AND APPLICATIONS IN ENGINEERING
ISSN:2147-6799 www.ijisae.org Original Research Paper

Detection of Spectrum Sensors for Maximizing Eigenvalue and Hardware Efficiency in Cognitive Radio Networks Using Machine Learning

K. Vadivelu[1]*, E. Gnanamanoharan[2], Dr. S. Tamilselvan[3]

Submitted: 17/07/2023 **Revised**: 09/09/2023 **Accepted**: 27/09/2023

Abstract: Cognitive radio networks (CRNs) make it possible for opportunistic spectrum access by dynamically identifying and utilising underutilised frequency bands. In this research, we provide a spectrum sensor architecture for CRNs that is hardware-efficient and based on simulated Maximum Eigenvalue Detection (MED). The suggested architecture makes use of MED, a dependable technique for locating signals in noisy situations. We address the resource limitations of actual CRN devices as we propose a hardware-efficient version of this detection algorithm. A combination of analogue and digital processing steps is used in the architecture. The signal that has been previously established undergoes initial filtration and amplification via the analogue front-end. Subsequently, it undergoes a conversion process from analogue to digital format. The next step in the digital processing stage is pre-processing, which includes feature extraction and noise removal. The covariance matrix (CM) is built using the retrieved characteristics, and the greatest eigenvalue is determined from this matrix. Offer a Simulated Maximum Eigenvalue Detection (SMED) method to increase hardware effectiveness. Employ a portion of the conventional signal illustrations to estimate the greatest eigenvalue rather than computing the whole covariance matrix. This maintains detection performance while substantially reducing computing complexity. Using effective parallel processing units and improved memory management, create a hardware architecture especially suited for the suggested approach. The architecture guarantees energy economy and real-time processing, which are essential for CRN devices with limited resources. Numerous simulations and comparisons with current spectrum sensing methods show how effective and efficient the suggested architecture is. Software from Xilinx was used to develop a hardware-efficient architecture with a fast spectrum sensor based on MED. The findings demonstrate that SMED-based spectrum sensors, which are hardware-efficient, can identify signals with high reliability while using a fraction of the resources. Spectrum sensing in CRNs is made simple and hardware-friendly by the suggested architecture. Because of its effective implementation, cognitive radio devices can use the spectrum more effectively, improving overall network performance

Keywords*: Eigenvalue Detection, Cognitive Radio Network, Triangular Systolic Array (TSA), Maximum Eigenvalue Detection (MED), Fusion Centre (FC), Empirical Mode Decomposition*

1. Introduction

The mandate for radio spectrum has risen substantially due to the fast expansion of diverse wireless communication applications, and it now appears to be very challenging to accommodate every new technology within an insufficient frequency spectrum due to the already highly constrained distribution of frequency resources. Because spectrum resources, which are essential to mobile communication, are currently underutilised, the development of wireless communication technology is significantly constrained [1-2]. In the post-5G era, planning and allocating spectrum resources will be crucial. A Cognitive Radio Network (CRN) has been suggested by some experts as a smart spectrum-sharing system to make the most of available spectrum because it is now being wasted mainly in terms of time and space [3]. Unlicensed or secondary users (SU) are given opportunistic spectrum access through CRN, which has lately become recognised as a novel technique for enhancing spectrum utilisation. CR is capable of detecting both a particular portion of the spectrum and a wide variety of its surroundings. The successful detection of the spectrum is therefore the most important first step for cognitive radio systems. Numerous strategies based on single threshold techniques are suggested to achieve successful spectrum sensing performance. As a result of low SNR, unpredictable noise, and multi-path fading, single-threshold techniques can perform poorly. These problems are addressed by the introduction of double-threshold spectrum sensing techniques, which further increase the likelihood of detection even at low SNR levels [4-5].

The two main categories of traditional spectrum sensing methods are narrowband and wideband methods. Wideband sensing simultaneously analyses numerous

[1] Research Scholar, Department of ECE, Faculty of Engineering & Technology, Annamalai University, Annamalai Nagar, Chidambaram. Email ID: vadivelecepan@gmail.com*
[2] Assistant Professor, Department of ECE, Faculty of Engineering & Technology,
Annamalai University, Annamalai Nagar, Chidambaram. Email ID: gnanamanohar@gmail.com
[3] Professor, Department of ECE, Puducherry Technological University, Kalapet, Puducherry.
Email ID: tamilselvan@ptuniv.edu.in

frequencies, as opposed to narrowband sensing's single-frequency channel focus. Instances of the former comprise energy detection, covariance-based detection, matching filter detection, cyclostationary features detection, and ML-based sensing. The spectrum is then regularly divided into numerous sub-bands, which are then detected using narrowband sensing techniques, either successively or concurrently [6–8]. However, a common issue with conventional spectrum sensing or detection methods is noise uncertainty. At low SNR, noise barriers exist, severely impairing the presentation of the detector. As a result, when using spectrum sensing devices that are vulnerable to noise uncertainty, CNR may interfere with Primary User (PU) communication at low SNR [9]. Despite the additional hardware complexity and sensing time, cyclostationary detection-based spectrum sensing methods perform well for strongly correlated signals at lower SNR [10]. Therefore, to address this issue, a sensor of the spectrum that is more hardware efficient, has faster sensing times, and performs better even in the worst channel conditions must be created. Image processing, audio identification, radio signal classification, and natural language processing are just some of the many fields that have found success with deep learning [11]. In this paper, we reformulate spectrum sensing as a two-class classification issue and solve it using a deep convolutional neural network (CNN). To perform eigenvalue-based spectrum sensing, in-depth background knowledge of the primary user signals and noise power is unnecessary. Using random-matrix theory, researchers tested hypotheses and settled on cutoff values for eigenvalue-based spectrum measuring methods [12]. The test statistic used to identify the presence or absence of the principal user indication is obtained by calculating the ratio between the greatest or median eigenvalue and the lowest eigenvalue. This test statistic is then compared to a decision threshold. The considerable operational complexity of this system, however, is a drawback. If the precise material about the PUs is unknown, eigenvalue detection-based approaches are employed instead [13]. These approaches have little mathematical and hardware complexities.

The primary heavy force behind the current endeavour is the issue of obtaining sufficient precision while having a quick sensing time. This issue represents a significant technological hurdle that must be overcome to build a wideband sensing strategy that is computationally modest. Future wideband spectrum usage is anticipated to be more efficient thanks to CRN, with signals expected to fill several sub-bands. Compressed sensing could fail as a result of the non-sparsity. Ineffective compressed sensing may also emerge from wideband operation with a variable noise floor due to low SNR and noise uncertainty. It is vital to change both the hardware and the environment as communication technologies advance from 5G to 6G. Existing approaches to spectrum sensing for CRN must incorporate artificial intelligence elements [14–15]. For resolving the spectrum scarcity issue, a quick and efficient spectrum sensing paradigm is preferred for MED spectrum sensors. Following is the arrangement of the remaining sections: Section 2 included a review of the literature; Section 3 the identification and motivation of the study's problems; Section 4 the recommended technique; Section 5 discussion of the results; and Section 6 the paper's conclusion.

2. Literature Survey

The great recital of eigenvalue-based detectors in SU detection in CRN has attracted a lot of interest. In order to enhance the efficacy of detection, Giri and Majumder et al [16] developed a cooperative spectrum sensing (CSS) technique that relies on eigenvalues and employs Kernel fuzzy c-means (KFCM) clustering. The test vectors obtained from the constrained eigenvalues are categorized into distinct clusters based on the availability and unavailability of channels using clustering techniques in two-dimensional or three-dimensional space. This approach deviates from existing systems that rely on a singular test statistic inside a solitary dimension to make sensing judgments. In their study, Du et al. [17] introduced the Average Circulant Matrix (CM) -based Roy's Largest Root Test (ACM-RLRT) and ACM-based Generalized Likelihood Ratio Test (ACM-GLRT) detectors. The covariance matrix of the samples from the statistical units (SUs) at each specific time instant is computed, and afterwards, the covariance matrix of the SUs is averaged over a short duration. The detectors are constructed using the obtained ACM Eigenvalues. Even with short samples, utilizing a CM can increase the covariance matrix's dominant eigenvalue of signals, as well as the detection efficiency. It is, nonetheless, a necessary process that has the highest influence on the reliability of CRNs. Therefore, Chaurasiya *et al* [18] focused on the CSS in VLSI architecture. CSS is a modern method of determining spectrum possession by licenced users in the CRN. The CRN, which is based on data fusion, employs CSS algorithms that apply maximum-minimum eigenvalue (MME) and maximum eigenvalue (MED) approaches to calculate the maximum and minimum eigenvalues inside the MME and MED algorithms. Liu *et al* [19] introduced a space-air-ground integrated network (SAGIN) for high-area connections. While advances in allowing access to the dynamic spectrum demonstrate potential in advancing higher spectrum sensing sharing, one of the fundamental issues encountered by spectrum management is dependable spectrum sensing below low SNR. To enhance the performance of sensing, deep learning-based spectrum sensing has been developed utilizing the concepts of data mining. On the basis of the covariance matrix of the

received signal vector, Jie et al. (2020) presented three high-performance detectors for determining the survival of a single passive emitter. This concept draws inspiration from detection principles used in radio discovery and radar systems. The MME and MED algorithms are used to develop the framework. The ratio test achieves less than 0.3 false alarm probability. However, in cognitive radio systems, there is a spectrum sensing problem that can be handled by by means of multi-input and multi-output (MIMO).

Al-Amidie *et al* [21] investigated the estimation and detection structure for the MIMO system with faultless channel state evidence where the NCM is unknown. In cognitive radio, GLRT was utilised to solve the spectrum sensing problem when the NCM was unknown and had imperfect channel data. The proposed approach delivers the greatest performance under stated assumptions, as shown by the results. In order to achieve a hybrid Spectrum sensing solution in CRN, Nasser et al. [22] suggested using ANN. Data can be characterised as tabular because it is made up of the test statistics of numerous detectors. The most appropriate ANN model is fully connected neural networks. To achieve an accurate solution, a cutting-edge deep learning technique was utilized for spectrum sensing. In implantable medical devices (IMDs), one of the design issues is the power need, which must be kept to a bare minimum to avoid repeated battery replacements and procedures. Therefore, Biswas and Mahbub *et al* [23] demonstrated a duty-cycled IR-UWB transmitter that achieves energy efficiency using a typical 180 nm CMOS technology. The proposed transmitter's wide frequency and bandwidth range make it ideal for distributed brain transplant applications in UWB higher and lower frequency bands. Soundararaj *et al* [24] used the NI-USRP hardware platform to introduce a CSS-based eigenvalue scheme and achieved good efficiency. The PU is a transmitter, which is implemented in hardware utilizing two cognitive radio users. In their study, Feng et al. (25) proposed a novel approach in the field of cognitive unmanned aerial vehicle networks (CUAVNs) to enhance spectrum utilization. This approach involves the use of a continuous hidden Markov model (CHMM) in conjunction with a distinctive signal-to-noise ratio (SNR) estimation method, as suggested by the authors. Furthermore, the authors drew inspiration from signal reconstruction on graphs to enhance the suggested sensing system based on the Continuous Hidden Markov Model (CHMM). This enhancement specifically addresses the issue of erroneous Signal-to-Noise Ratio (SNR) estimates in real-world applications. According to simulation findings, the sensing technique based on projected Continuous Hidden Markov Models (CHMM) has superior performance compared to methods that do not use CHMM. Furthermore, the CHMM-based sensing strategy, when combined with the recommended Signal-to-Noise Ratio (SNR) estimator, exhibits a considerable improvement over the traditional approach[26-30].

3. Research Problem Definition and Motivation

Due to its precision and dependability, cooperative spectrum sensing (CSS), a family of well-known approaches in the spectrum detecting field, has lately garnered significant attention. Many CSS approaches based on random matrix (RM) theory have been described, in which the Fusion Centre (FC) assembled the signal vectors from all of the SUs into a signal matrix and calculated the appropriate covariance matrix. In this situation, an amount of spectrum sensing schemes have been put forth over the past few years. Among these methods are energy-based detectors (EBD), eigenvalue-based spectrum sensing, matched-filter detection covariance, and cyclostationary - based spectrum sensing. The EBD methods are typically straightforward to use, but they also call for an understanding of the noise variability that is involved. For certain signal categories, the EBSS approaches, in particular the MMED and GLRT, may operate without being aware of the variance in noise and provide noticeably better performance.

Spectrum prediction, signal categorization, signal enumeration, spectrum handover, etc. are just some of the cognitive radio applications that have found success using machine learning (ML) approaches. A feature vector is taken from the signal and sent to the classifier in order to conduct spectrum sensing. The signal is then split by the classifier into classes of accessible and unavailable channels. Several well-known machine learning (ML) techniques include support vector machines (SVM), neural networks, and various clustering techniques. The training and inference durations of CSS have been decreased because to the usage of an extreme learning machine (ELM), a kind of neural network. There have been several attempts to solve the CSS problem by using various clustering techniques. The dominating eigenvalue, the maximum eigenvalue, and the MEV from a sensing signal CM were formed into signal feature vectors, which are then utilised to train the classifier for spectrum sensing. In a real-world situation, noise and sensing speed contaminate the gathered sensory data, lowering the routine of detection. This drives the development of a maximum eigenvalue-based detection system, which will reduce noise sources and enhance detection efficiency.

4. Proposed Research Methodology

The crucial technique of spectrum sensing largely impacts the dependability of CRNs. The modern method for determining if licenced users are using spectrum in CRN is CSS. The traditional stand-alone spectrum-sensing (SSS)

methods are outperformed by this one. However, compared to SSS algorithms, such CSS algorithms require a more sophisticated implementation, which increases resource usage and decreases hardware efficiency. Therefore, the focus of the study is on developing a MED-based CSS algorithm that runs efficiently on a VLSI hardware architecture. Figure 1 is a flowchart depicting the planned process.

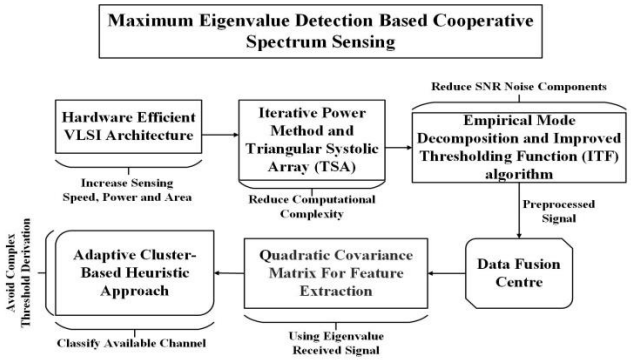

Fig. 1: Flow Chart of the Proposed Work

The suggested work's block diagram is shown in Figure 1. Technology-dependent optimal VLSI architecture necessitates the characterisation of key functional units for power, area, and speed. The MED computation is performed using the TSA architecture, which is based on the iterative power approach. To eliminate the noise components included in the spectrum sensing signal, the initial step involves pre-processing the identified primary user (PU) signal at secondary users (SUs) via the use of the Empirical Mode Decomposition (EMD) and Improved Thresholding Function (ITF) algorithms. The eigenvalues of the covariance matrix (CM) of the received signal are used as attributes for detection in the feature extraction process at the fusion center (FC) by using the pre-processed signal. A quadratic CM of cooperative SUs serves as the characteristic matrix for feature extraction. The features are chosen according to their maximum eigenvalues to construct a dimensional feature vector. The research proposed the use of a Modified Adaptive Cluster-Based Heuristic Approach (MACBHA) in spectrum sensing, based on the identified characteristics. This decreases the requirement for complex threshold computation while increasing detection performance.

(a) VLSI Architecture of MED-Based Spectrum Sensor

Recent research has introduced a hardware-efficient layout with a fast spectrum sensor based on MED. Our talks will initially center on this setup, which we will describe to as a "standard MED-based spectrum sensor" for the duration of this research. Maximum eigenvalue computation & decision module, covariance-matrix creation module, and auto-correlation computation module are the three primary modules of a traditional MED sensor. This typical MED sensor architecture has been further optimised by us and is shown to you in this part. Choosing the right initial vector $\boldsymbol{x^k}$ and taking advantage of the symmetry of the $\boldsymbol{y^k}$ matrix, the computation of the lower $\boldsymbol{L/2}$ rows of the $\boldsymbol{y^k}$ the matrix can be derived from the upper L/2 rows of the $\boldsymbol{R_x}$ $(\boldsymbol{Ns})$ matrix. This computation can be done by ACM and CFM architectures. One suggests employing only $\boldsymbol{L/2}$ commotions of the matrix $\boldsymbol{R_x}$ $(\boldsymbol{Ns})$ rather than the $\boldsymbol{L}$ rows used in the traditional MED spectrum sensor to compute y kof size $\boldsymbol{L \times 1}$. This optimisation reduces the hardware requirements of the CFM and MECDM in the traditional MED design while also speeding up the sensing process. For the sake of clarity, assume that $[\widehat{\boldsymbol{R}}_{\boldsymbol{x}}(\boldsymbol{Ns})]_{4\times4}$ and $[\boldsymbol{x^{k-1}}]_{4\times1}$are both true for $\boldsymbol{L = 4}$. Consequently, the matrix $[\boldsymbol{y^k}]_{4\times1}$ is calculated as

$$\boldsymbol{y^k} = \begin{bmatrix} \boldsymbol{a} & \boldsymbol{x+iy} & \boldsymbol{c+id} & \boldsymbol{m+in} \\ \boldsymbol{x-iy} & \boldsymbol{a} & \boldsymbol{x+iy} & \boldsymbol{c+id} \\ \boldsymbol{c-id} & \boldsymbol{x-iy} & \boldsymbol{a} & \boldsymbol{x+iy} \\ \boldsymbol{m-in} & \boldsymbol{c-id} & \boldsymbol{x-iy} & \boldsymbol{a} \end{bmatrix} \times \begin{bmatrix} \boldsymbol{1} \\ \boldsymbol{1} \\ \boldsymbol{1} \\ \boldsymbol{1} \end{bmatrix} \quad (1)$$

$$\boldsymbol{y^k} = \begin{bmatrix} \boldsymbol{(a+x+c+m)+i(n+y+d)} \\ \boldsymbol{(x+a+x+c)+i(d)} \\ \boldsymbol{(x+a+x+c)-i(d)} \\ \boldsymbol{(a+x+c+m)-i(n+y+d)} \end{bmatrix} \quad (2)$$

The elements of the $\boldsymbol{y^k}$ matrix's bottom half third and fourth rows are complex conjugates of those in the third and first rows in the upper half, respectively. Consequently, it is sufficient to use just the top half of the elements in the matrix 〖Rˆ〗_x (Ns) for the construction of both 〖y 〗^k and 〖x 〗^k. The proposed modification to the architecture of the MED spectrum sensor involves the construction of the 〖Rˆ〗_x (Ns) matrix using just a subset of components from L/2 rows, rather than using all L rows (where L = 8 in our specific design). Consequently, the CFM and MECDM designs that have been suggested exhibit reduced area overhead and routing complexity. The new CFM architecture uses three complex conjugate modules (CCMs) as opposed to seven CCMs and a 4:1 multiplexer in place of an 8:1 multiplexer found in the standard CFM module from [20]. The multiplexer size has been decreased from 8:1 to 4:1, and both of the MECDM architecture's 1:8 de-multiplexers have been converted to their respective 4:1 variants. Furthermore, compared to the six MAX modules required by a traditional MED sensor, MECDM only requires three MAX modules.

(i) Triangular Systolic Array (TSA)

The power method-based eigenvalue computations-based proposed hardware-efficient MME algorithm has been provided. Referring, the CM is created by computing the autocorrelation of the signal that was received. The suggested power approach for calculating the maximum eigenvalue is shown in lines. In order to ensure that the beginning vector does not align with the non-dominant

vector, it is chosen as an arbitrary L×1 vector with elements equal to '1' in this particular scenario. In the traditional power technique, this calculation is made as $\boldsymbol{\mu_k = max\left[abs\left(y^{\,k}\right)\right] = max\sqrt{(\Re\{y^{\,k}\})^2 + (\Im\{y^{\,k}\})^2}}$, requiring a square-root computation unit in addition to the squarer and adder blocks. However, the suggested optimisation just needs to access the true portion of $\boldsymbol{y^{\,k}}$.

The algorithm's performance was only slightly harmed as a result, and a detailed overview of it is now offered. The greatest eigenvalue is then discovered. The least eigenvalue of an arbitrary square matrix $[\boldsymbol{A}]_{\boldsymbol{N\times N}}$ may be determined using the inverse power technique or the shift power method. It can be seen that the contrary of the matrix being considered must be determined for the converse power approach, which increases the complexity of hardware realisation. Additionally, this inverse matrix has a maximal eigenvalue that must be found using the power approach. Matrix B may be generated by using the largest eigenvalue of matrix A by the use of the shift Power Method (PM) as outlined in Algorithm 3. The resulting matrix B will exclusively consist of negative eigenvalues. Moreover, the principal method (PM) is used for the computation of the eigenvalue, namely the one with the greatest magnitude and most negative value, of matrix B. The lowest eigenvalue of matrix A may be found by adding the biggest eigenvalue of matrix A to the eigenvalue of matrix B. It should be noted that the shift PM only works with positive definite matrices.

(ii) Maximum Eigenvalue Detection (MED)

The core issue in binary hypothesis testing is in the distinction between the H_0 and H_1 hypotheses, which alternately represent the absence and presence of the primary user (PU) signal. This constitutes the essential framework for spectrum sensing. They are stated mathematically as

$$\boldsymbol{H_0: x[n] = \eta[n]} \quad (3)$$

$$\boldsymbol{H_1: x[n] = h[n].s[n] + \eta[n]} \quad (4)$$

$\forall\, \boldsymbol{n = \{1, 2, 3, \ldots\ldots N_s\}}$ where, $\boldsymbol{N_s}$ represent the total number of samples used for detection. The sent signal sample of the primary user PU is denoted as s[n], whereas η[n] represents the noise sample. The frequency-flat channel response is represented by h[n], and x[n] is the received sample or observation. The computation of the test statistics value (·) is conducted using the recorded observations and afterwards compared to the standard decision-threshold value γ, which determines the existence or absence of a particular phenomenon of PU$\{\boldsymbol{i.e.(x[n]\ \forall\, n = 1, 2, \ldots, Ns) \lessgtr H0\ H1\ \gamma}\}$ in relation to the hypotheses H0 and H1. In this section, we will sequentially provide the theoretical foundations of Spectrum Sensing Algorithms (SSA) that are based on Minimum Eigenvalue Detection (MED), Energy with Minimum Eigenvalue (EME), and Mean-to-Square Extreme Eigenvalue (MSEE). The Maximum Eigenvalue Detector (MED)-based spectrum sensing method is well-suited for analyzing correlated received-signal samples. This approach involves first calculating the auto-correlation of the samples denoted as x[n].

$$\boldsymbol{\lambda(l) = \frac{1}{N_s}\sum_{m=0}^{N_s} x*[m].x[m-l], \forall\, l = \{0, 1, \ldots l-1\}} \quad (5)$$

Where $\boldsymbol{L}$ is the lag/smoothing factor. Subsequently, the sample covariance matrix of such auto-correlated values is constructed as

$$\boldsymbol{\widehat{R}_x\,(N_s) = \begin{bmatrix} \lambda(0) & \lambda(1) & \cdots & \lambda(L-1) \\ \lambda*(0) & \lambda(0) & \cdots & \lambda(L-2) \\ \vdots & \vdots & \vdots & \vdots \\ \lambda*(L-1) & \lambda*(L-2) & \cdots & \lambda(0) \end{bmatrix}} \quad (6)$$

This is the Hermitian-Toeplitz matrix whose maximum eigenvalue, represented as $\boldsymbol{\lambda_{max}}$, is the test statistics value for MED-based SSA (i.e. $\boldsymbol{\Gamma_{MED} = \lambda_{max}}$). The decision threshold value, which is given as $\boldsymbol{\gamma MED = \gamma \cdot \sigma^2}$, is pre-calculated with unity noise variance (i.e. $\boldsymbol{\sigma^2 = 1}$) as

The function F^{-1} represents the cumulative distribution function of the Tracy-Widom distribution with an order of 1, while $\boldsymbol{P_{fa}}$ is the probability associated with a false alarm. The aforementioned threshold value is then compared with $\boldsymbol{\Gamma_{MED}}$ in order to determine the existence or absence of PU, as previously explained. The efficacy of the MED algorithm's detection capability is contingent upon the presence of noise variance and noise uncertainty, both of which are inherent in real-world scenarios and may detrimentally impact its performance. The real-time calculation of noise variance, which is practically unfeasible, is necessary to provide accurate identification of primary users (PUs) via the use of the Minimum Energy Detector (MED) method.

The EME-based SSA, as suggested by the test statistics value, involves the computation of the ratio between the energy of received signal samples, x[n] ∀ n={1, 2, 3, ... $\boldsymbol{N_s}$} and the minimum eigenvalue ($\boldsymbol{\lambda_{min}}$) of sample CM $\boldsymbol{\widehat{R}_x\,(N_s)}$, as given below

$$\boldsymbol{\Gamma_{EME} = \left(\frac{\frac{1}{N_s}\sum_{N=0}^{N_s-1}|X[n]|^2}{\lambda_{min}}\right)} \quad (8)$$

Furthermore, it should be noted that the determination threshold for spectrum sensing based on Energy Detection (EME) is unaffected by variations in noise variance, hence indicating its independence from uncertainties introduced by noise.

(b) Empirical Mode Decomposition (EMD)

Assuming $\boldsymbol{xi} = [\boldsymbol{xi}(\mathbf{1})\boldsymbol{xi}(\mathbf{2}), \ldots, \boldsymbol{xi}(\boldsymbol{N})]$, the sample vector of the *i*th secondary user (SU) is denoted as represents. In order to mitigate the impact of noise on the spectrum sensing system, the present study employs the EMD method as a pre-processing technique for the spectrum signal. The signals throughout the spectrum exhibit non-stationarity and non-linearity within their respective environments. Conventional signal processing methods, such as Fourier transforms, wavelet transforms, and others, are applicable only to signals that possess linear stability. This study introduces the EMD method to achieve a better clustering result. EMD can effectively process non-linear signals and non-stationary as compared to conventional signal processing techniques.

The EMD technique primarily aims to partition the signal into many intrinsic modal function components (IMFs) arranged in descending order of frequency. Assume that the spectrum signal is $\boldsymbol{x_i(n)}$. After EMD decay, the signal $\boldsymbol{x_i(n)}$ may be stated as:

$$\boldsymbol{x_i(n)} = \sum_{j=1}^{j} \boldsymbol{IMF_j(n)} + \boldsymbol{r(n)} \quad (9)$$

$\boldsymbol{r(n)}$ is a representation of the residual.

The following are the precise stages in the EMD decomposition process:

Step 1*:* Find the spectrum signal's regional lowest and maximum values. $\boldsymbol{x_i(n)}$.

Step 2: Find the maximum envelope $\boldsymbol{x_i^{max}(n)}$ and minimum envelope $\boldsymbol{x_i^{max}(n)}$ in the spectrum signal $\boldsymbol{x_i(n)}$. And then compute their average $\boldsymbol{m_1(n)}$.

$$\boldsymbol{m_1(n)} = \frac{\boldsymbol{x_i^{max}(n) - x_i^{min}(n)}}{\mathbf{2}} \quad (10)$$

Step 3: Obtaining the $\boldsymbol{h_1(n)}$ component using equation (11)

$$\boldsymbol{h_1(n)} = \boldsymbol{x_i(n)} - \boldsymbol{m_1(n)} \quad (11)$$

Check to see whether $\boldsymbol{h_1(n)}$ satisfies the IMF's two requirements. Once satisfied, go to

Step 4: If not, repeat Steps 1 and 2 until the IMF requirements are satisfied. In order to determine the IMF component, use equation (12).

$$\boldsymbol{IMF_1} = \boldsymbol{h_1(n)} \quad (12)$$

Step 5: Making the residual calculation using equation (13)

$$\boldsymbol{h_1(n)} = \boldsymbol{x_i(n)} - \boldsymbol{IMF_j(n)} \quad (13)$$

Treat $\boldsymbol{r_1(n)}$as the original signal and repeat Steps 1-5 to get $\boldsymbol{r_2(n)}$. And so on until the residual $\boldsymbol{r_J(n)}$is a monotonous function or a constant.

Real-world perceptual environments often include high-frequency band (HFB) noise and low-frequency band (LFB) usable signal concentrations. To minimize certain high-band noise signals and then rebuild the low-frequency signals is the basic idea behind EMD denoise. According to the continuous mean square error criteria, the low-frequency band and HFB critical point. Due of the expression's clarity, let $\tilde{\boldsymbol{y}}$ represent $\boldsymbol{x_i(n)}$.

$$\boldsymbol{CMSE(\tilde{y}m, \tilde{y}m + 1)} = \frac{\mathbf{1}}{\boldsymbol{N}} \sum_{\boldsymbol{n=1}}^{\boldsymbol{N}} \boldsymbol{(\tilde{y}m - \tilde{y}m + 1)^2}$$

$$= \frac{\mathbf{1}}{\boldsymbol{N}} \sum_{\boldsymbol{n=1}}^{\boldsymbol{N}} \boldsymbol{(IMF_n(n)^2)} \quad (14)$$

$$\boldsymbol{m} = \boldsymbol{argmin}[\boldsymbol{CMSE(\tilde{y}m, \tilde{y}m + 1)}](\mathbf{1} \leq \boldsymbol{m} \leq \boldsymbol{J} - \mathbf{1}) \quad (15)$$

After all the signals collected by the M SUs are processed by the EMD denoising process, the processed signals can form a new signal matrix $\boldsymbol{Y} = [\tilde{\boldsymbol{x}}\mathbf{1}, \tilde{\boldsymbol{x}}\mathbf{2}, \ldots, \tilde{\boldsymbol{x}}\boldsymbol{M}]^{\boldsymbol{T}}$, where $\tilde{\boldsymbol{x}}_{\boldsymbol{i}} = \tilde{\boldsymbol{x}}_{\boldsymbol{i}}\mathbf{1}, \tilde{\boldsymbol{x}}_{\boldsymbol{i}}\mathbf{2}, \ldots . \tilde{\boldsymbol{x}}_{\boldsymbol{i}}\boldsymbol{N}$ represents the signal acquired by the $\boldsymbol{i}$th noise-reduced SU by the EMD. Therefore, $\boldsymbol{Y}$ is a $\boldsymbol{M} \times \boldsymbol{N}$ dimension matrix

$$\boldsymbol{Y} = [\tilde{\boldsymbol{x}}\mathbf{1}, \tilde{\boldsymbol{x}}\mathbf{2}, \ldots, \tilde{\boldsymbol{x}}\boldsymbol{M}]^{\boldsymbol{T}} = \begin{bmatrix} \tilde{\boldsymbol{x}}_{\mathbf{1}}(\mathbf{1}) & \tilde{\boldsymbol{x}}_{\mathbf{1}}(\mathbf{2}) & \cdots & \tilde{\boldsymbol{x}}_{\mathbf{1}}(\boldsymbol{N}) \\ \tilde{\boldsymbol{x}}_{\mathbf{2}}(\mathbf{1}) & \tilde{\boldsymbol{x}}_{\mathbf{2}}(\mathbf{2}) & \cdots & \tilde{\boldsymbol{x}}_{\mathbf{2}}(\boldsymbol{N}) \\ \vdots & \vdots & \ddots & \vdots \\ \tilde{\boldsymbol{x}}_{\boldsymbol{M}}(\mathbf{1}) & \tilde{\boldsymbol{x}}_{\boldsymbol{M}}(\mathbf{2}) & \cdots & \tilde{\boldsymbol{x}}_{\boldsymbol{M}}(\boldsymbol{N}) \end{bmatrix} \quad (16)$$

Order-DAR (O-DAR) and interval-DAR (I-DAR) were introduced to increase the sensing performance in the case of fewer cooperating SUs after the original signal was denoised by the EMD method. Logically, the approach can boost spectrum sensing efficiency and the quantity of cooperative SUs.

(i) Improved Thresholding Function (ITF)

The nonlinear and noisy data are divided using soft threshold (ST), hard threshold (HT), and improved threshold function (ITF) for evaluation of EBT with additional thresholding approaches. For soft, hard, and upgraded thresholds, the following mathematical formulations are provided:

$$\boldsymbol{c'_{x,l}} = \{\boldsymbol{d_{x,l}}|\boldsymbol{c_{x,l}}| \geq \boldsymbol{Th_l}\mathbf{0}|\boldsymbol{c_{x,l}}|\langle \boldsymbol{Th_l}\rangle, \quad (17)$$

$$\boldsymbol{c'_{x,l}} = \{\boldsymbol{sgn(c_{x,l})}(|\boldsymbol{c_{x,l}}| - \boldsymbol{Th_l})|\boldsymbol{c_{x,l}}| \geq \boldsymbol{Th_l}\mathbf{0}|\boldsymbol{c_{x,l}}|\langle \boldsymbol{Th_l}\rangle, \text{ and}$$

$$\boldsymbol{c'_{x,l}} = \{\boldsymbol{sgn}(\boldsymbol{c_{x,l}})|\boldsymbol{c_{x,l}}| - \frac{\boldsymbol{Th_l}}{[\boldsymbol{\alpha}|\boldsymbol{c_{x,l}}| - \boldsymbol{Th_l}/\boldsymbol{Th_l}]}, |\boldsymbol{c_{x,l}}|\langle \boldsymbol{Th_l}\rangle, \quad (18)$$

Where, $\boldsymbol{Th_l}$is the threshold which is calculated as $\boldsymbol{Th_l} = \boldsymbol{a}\sqrt{\mathbf{2}\boldsymbol{E_l}}\boldsymbol{In(N)}, \boldsymbol{l} = \mathbf{1}, \mathbf{2}, \mathbf{3}, \ldots \boldsymbol{L}$, where $\boldsymbol{a}$ is constant which considers the values between 0.4 and$\widehat{\boldsymbol{Md_l}}$is the median deviation, that is, $\widehat{\boldsymbol{Md_l}}$ =median($\{\boldsymbol{c_{l-1}l} = \mathbf{1}, \mathbf{2}, \mathbf{3}, \ldots, \mathbf{2^{l-1} - 1}\}$)$/\mathbf{0.6745}$

(ii) Fusion Centre (FC) For Feature Extraction

The pre-processed signal is directed to the fusion centre (FC) for additional examination and decision-making after being collected from a source or sensor. In the FC, one of the crucial processes is feature extraction, in which pertinent data is taken from the signal that has been received to help with tasks like detection or classification. The feature extraction procedure in this instance entails calculating the eigenvalues of the CM of the conventional signal. The CM offers details on the statistical correlations and variances between various signal constituents or properties. We can determine the eigenvalues of this matrix and deduce important properties that describe the structure and variability of the signal. When the CM is multiplied by the associated eigenvectors, eigenvalues describe the scaling factors that are applied to those eigenvectors. They communicate important details about how the data are dispersed and distributed. The eigenvalues of the CM can be used as discriminative features to help discriminate between various classes or states of the signal in the context of feature extraction.

The eigenvalues can be utilised as characteristics for detection. The eigenvalues can capture unique characteristics of the received signal that are indicative of the target class, for instance in a binary classification issue where the objective is to sense the existence or absence of a particular signal or event. The fusion centre can identify whether or not the desired signal is present by comparing the extracted eigenvalues to specified thresholds or by applying a statistical decision procedure. The fusion centre can efficiently extract pertinent information from the pre-processed signal by using the eigenvalues as features, allowing accurate detection or classification of the fundamental phenomenon of interest. This method improves the fusion centre's decision-making process by taking advantage of the statistical properties of the established signal.

(iii) Quadratic Covariance Matrix

The distinguishing matrix for feature extraction on a cooperative network of secondary users (SUs) is defined as the quadratic covariance matrix. The statistical correlations and variances between the various characteristics or aspects of the data from the cooperative SUs are captured in this matrix. The square matrix of size $\boldsymbol{N\,x\,N}$ that makes up the quadratic covariance matrix, abbreviated as $\boldsymbol{C}$, is equal to the number of features or dimensions in the data. The covariance between the $\boldsymbol{i-th}$ and $\boldsymbol{j-th}$ features is represented by the $(\boldsymbol{i},\boldsymbol{j})$ −th element of the matrix $\boldsymbol{C}$. We choose features based on their maximum eigenvalues to generate a dimensional feature vector since $\boldsymbol{C}$ is a symmetric covariance matrix, meaning $\boldsymbol{C}(\boldsymbol{i},\boldsymbol{j}) = \boldsymbol{C}(\boldsymbol{j},\boldsymbol{i})$.

The spread and distribution of the data from the cooperative SUs throughout each dimension are shown by the eigenvalues of the covariance matrix $\boldsymbol{C}$. The scaling factors that are applied to the appropriate eigenvectors when C is multiplied by them are represented by the eigenvalues, indicated as $\boldsymbol{\lambda_1,\lambda_2,\ldots,\lambda_N}$. Pick the eigenvectors linked to the biggest eigenvalues to choose the features based on maximal eigenvalues. The most important directions of variation in the data from the cooperative SUs are captured by these eigenvectors. may create a feature vector that keeps the most crucial information while lowering dimensionality by choosing features that are aligned with these dominant eigenvectors. The dimensional feature vector, denoted as $\boldsymbol{F}$, is a column vector of size $\boldsymbol{M\,x\,1}$, where $\boldsymbol{M}$ represents the number of selected features. Each element of the feature vector, $\boldsymbol{F}(\boldsymbol{i})$, corresponds to the i-th selected feature. The selection of features is contingent upon their maximum eigenvalues, hence the features are chosen in decreasing order based on their connected eigenvalues. The equation provided may be used to generate a dimensional feature vector by considering the maximum eigenvalues:

$$\boldsymbol{F} = [\boldsymbol{f_1},\boldsymbol{f_2},\ldots,\boldsymbol{f_M}]\widehat{\boldsymbol{T}} \qquad (19)$$

Where, $\boldsymbol{f_1}$represents the $\boldsymbol{i}$-th selected feature, and $\boldsymbol{T}$ denotes the transpose operation. Overall, by utilizing the quadratic CM and selecting features based on their maximal eigenvalues, we can effectively extract the most significant information from the cooperative SUs' data and construct a dimensional feature vector that captures the essential characteristics of the system.

(c) Adaptive Cluster-Based Heuristic Approach

The information geometry-based MAC-BHA in multidimensional vector space is a technique used for spectrum sensing, whereby features are extracted from the data and educated judgments are made on the presence or absence of signals in the spectrum. This approach involves the creation of multidimensional vectors in the feature space by using the recovered features obtained through the aforementioned procedure. Every vector shows a particular occurrence or snapshot of the spectrum. To assess the connections and separations between these feature vectors and enable efficient spectrum sensing, the information geometry framework is then used. In the modified adaptive cluster-based heuristic technique, feature vectors are grouped or clustered according to their similarity. The process of clustering involves grouping or clustering data points so that they are more similar to one another than to those in other clusters. Let $\boldsymbol{C} = \{\boldsymbol{C1},\boldsymbol{C2},\ldots,\boldsymbol{Ck}\}$ be the set of clusters formed from the problem space. Each cluster Ci is defined by its centroid $\boldsymbol{\mu i}$ and its associated members $\boldsymbol{Mi}$. For each cluster $\boldsymbol{Ci}$ in $\boldsymbol{C}$, apply a heuristic algorithm to find a solution Si. Evaluate the solutions $\boldsymbol{Si}$ and update the performance measures. Based on the performance

measures, adapt the heuristic algorithm's parameters, search strategy, or cluster configuration.

The clustering procedure aids in locating structures or patterns in the data. The heuristic approach applies methods such as density-based clustering or k-means clustering to adaptively build clusters in the feature space. To establish suitable cluster borders, these approaches take into account the distribution and density of the feature vectors. To detect signals amid noise or interference, the clusters act as representations of various signal classes or states in the spectrum. This method's information geometry component focuses on the geometric characteristics of the feature space. Making more educated decisions about signal identification and extracting useful information about the spectrum is feasible by studying the distances, angles, and forms that the feature vectors generated. The feature space where the retrieved features are represented as vectors is referred to as the multidimensional vector space. The vectors collectively capture the fundamental properties of the spectrum at a specific instance, with each dimension of the vector correlating to a different aspect. Spectrum sensing is made more reliable and precise by using the information geometry-based MACBHA in this multidimensional vector space. The method makes use of the geometric characteristics of the feature vectors to locate clusters that represent various signal classes, enabling accurate signal detection and classification in the spectrum. This approach works especially well in situations where the spectrum is complicated and has a variety of signals and interference.

5. Experimentation and Result Discussion

For the cognitive radio networks (CRNs), we describe the outcomes of the hardware-efficient SMED-based spectrum sensor design in this section. The presentation of the suggested design was discussed, along with comparisons to other spectrum sensing methods, emphasising the benefits of the projected architecture in standings of hardware effectiveness and detection precision. The suggested architecture is deliberately made to be hardware-efficient, taking into account the resource limitations of actual CRN devices. We assess the architecture's resource use and hardware complexity, taking into account the needed power, memory, and computing units. The findings show that, as compared to conventional spectrum sensing methods, the suggested design significantly improves hardware efficiency. It is suited for use in CRN devices with limited resources because it strikes a compromise between accurate detection performance and reduced resource requirements. The energy detector-based sensing technique was implemented using VLSI architecture. The architecture implementation was studied and simulated using the simulator tool Xilinx 14.7. The results of the proposed circuit's synthesis are then taken into account in this section's timing analysis. The initial module design is done independently, while the final model implementation is done jointly. The suggested architecture of the energy detector was developed in Verilog, a standardised hardware description language. By doing so, it is decided whether the signal is present or not. The following is a presentation of the study's simulation results.

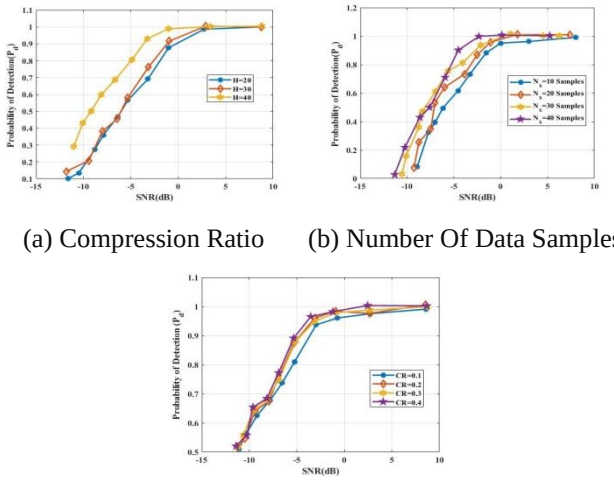

(a) Compression Ratio (b) Number Of Data Samples

(c) Filter Coefficients

Fig. 2: Comprehensive Performance Analyses of Proposed WSSR

It should be noted that the $\boldsymbol{P_d}$value is directly related to the channel signal-to-noise ratios (SNRs) and the power-to-load $\boldsymbol{P/L}$ compression ratio (CR). The compression ratio is a factor used in determining the decrease in multicast sampling frequency. The data clearly indicates a positive correlation between the value of the $\boldsymbol{P_d}$ and the CR value. Therefore, it can be inferred that the proposed Wideband Spectrum Sensing Receiver (WSSR) achieves improved detection performance at lower Signal-to-Noise Ratio (SNR) levels by using a higher Compression Ratio (CR) value together with a significant number of samples ($\boldsymbol{N_x}$) and coefficient values ($\boldsymbol{H}$). The performance analysis shown in Figure 2 (a) was conducted using a sample size of $\boldsymbol{N_x}$= 46 and a value of $\boldsymbol{H}$ = 383.In contrast, when the CR value is set at 0.36, p is equal to 8, and L is equal to 22, we have generated graphs depicting $\boldsymbol{P_d}$ vs SNR for different numbers of $\boldsymbol{N_x}$samples, ranging from 20 to 50 samples. These plots are shown in Figure 2 (b). The suggested weighted sum of squared residuals (WSSR) demonstrates satisfactory identification performance when using a sample size of $\boldsymbol{N_x}$ = 46.

However, any increase in sample size above this threshold only yields minimal improvements in performance.In addition, the sensing time of the serially linked ODS micro-architectures in the SD block of our WSSR increases as the value of $\boldsymbol{N_x}$ increases. Hence, a sample size of 46, denoted as $\boldsymbol{N_x}$, is deemed sufficient for

ensuring dependable performance and the development of a hardware-efficient architecture for the proposed WSSR. In a similar manner, the evaluation of its presentation has been conducted for different H coefficients of $\boldsymbol{h}[\boldsymbol{n}]$ values. This evaluation was performed using the parameters p = 8, L = 22, CR = 0.36, and $\boldsymbol{N}_{\boldsymbol{x}}$ = 50, as seen in Figure 2 (c). In this scenario, when the value of H is more than or equal to 40, the suggested WSSR method demonstrates constant performance, even when the signal-to-noise ratio (SNR) is reduced. Nevertheless, the incorporation of larger CS blocks and steering logic in our WSSR design will result in an extended sensing time.

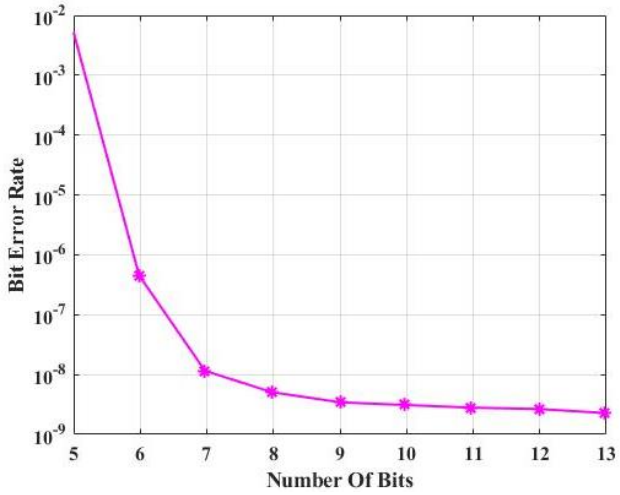

Fig. 3: Fixed-Point Simulation of IQRD with Different Word Lengths.

When the fractional word length surpasses 7 bits, the Bit Error Rate (BER) becomes saturated at a Signal-to-Noise Ratio (SNR) of 33 dB. Hence, it is advisable to use fractional words of 9 bits in hardware implementation. The architectural design in question employs an 18-bit representation for fractional operations and implements a truncation mechanism to reduce word lengths to 9 bits prior to output. This approach is used to solve the issue of overflow that may arise during the division process. Fixed-point simulation is also carried out to establish the ideal amount of bits for IQRD hardware implementation. The relationship between the use and word length is shown in Figure 3. The use of the fixed-point and floating-point QRD outputs represents the distinction between them. Figure 3 displays a saturated curve with a magnitude of 10 -8mse. The augmentation of bits does not enhance the system's appearance. Hence, it is feasible to create the hardware for the Integer Quotient and Remainder Division (IQRD) algorithm with a fractional word length of 9 bits.

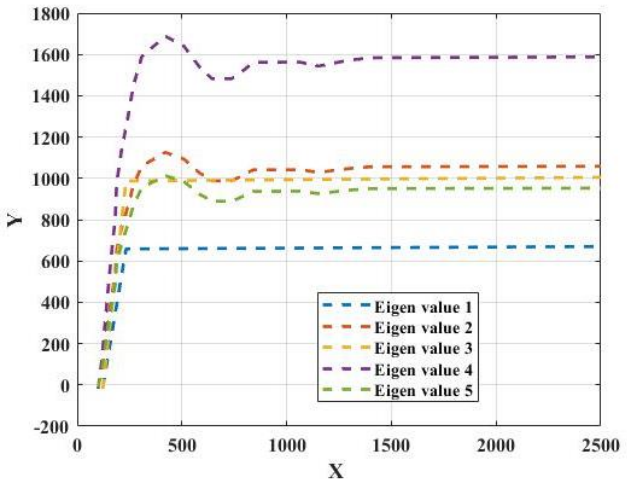

Fig.4: Convergence Analysis of Eigenvalues

The mean squared error (MSE) serves as a metric to quantify the discrepancy between the outputs of the floating-point and fixed-point QRD. Figure 3 displays a curve that is saturated, with a mean squared error of 10 -8. The enhancement in system performance is not achieved by increasing the number of bits. Hence, it is possible to use a 9-bit fractional word length throughout the process of building the IQRD hardware.

$$\boldsymbol{I} = \begin{bmatrix} \boldsymbol{O} & \boldsymbol{O} & \boldsymbol{-947 + i \times 699} \\ \boldsymbol{1103} & \boldsymbol{0} & \boldsymbol{306 - i \times 3139} \\ \boldsymbol{0} & \boldsymbol{1103} & \boldsymbol{2058 + i \times 2320} \end{bmatrix} \quad (20)$$

To the best of our knowledge, there isn't any published literature that can be used to compare our results, which are being used for the first time. While N is unrelated to the suggested design. Compared to previous architectures, this significantly reduces the design area of the algorithm.

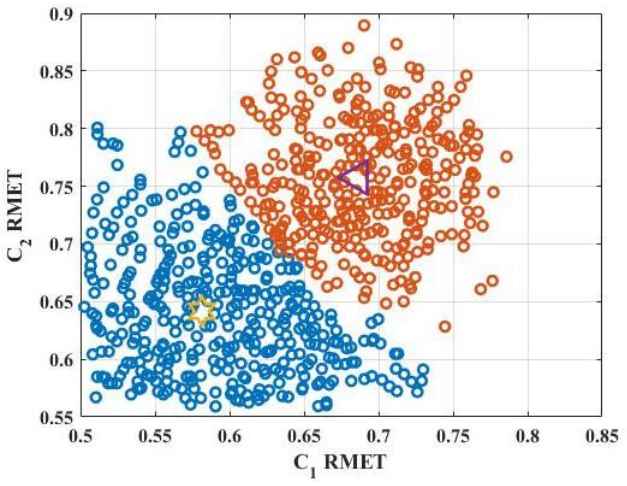

Fig. 5: Clustering Effect of the Ratios of the Maximum Eigenvalue

The mean squared error (MSE) serves as a metric to quantify the disparity between the outputs of the floating-point and fixed-point QRD algorithms. Figure 3 displays a curve that is saturated, with a mean squared error (MSE) value of 10^{-8}. The enhancement in system performance is

not achieved by increasing the amount of bits. Hence, it is possible to use a 9-bit fractional word length during the hardware construction of the IQRD.

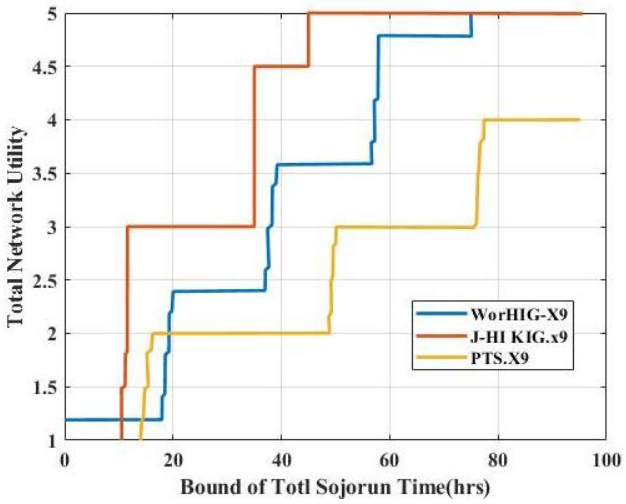

Fig. 6: Analysis of Network Utility and Time

Figure 6 demonstrates how as sojourn time rises, so does network utility. It indicates that as time goes on, the cluster's performance remains constant and effective. Every node will participate sporadically with time-limited access to the network. The stages for network utility remain the same when the time approaches a greater limit. It means that even when the length of time needed for data collection increases the network's data, it will still be used without any data loss.

(a) Comparison Analysis

The different strategies are compared and analysed for the best method as part of the comparative analysis that supports the proposed method. The assessment and evaluation of the comparisons and alterations among two or more subjects, objects, concepts, or things are done methodically using comparative analysis. This analytical method is frequently used in a variety of fields, including ROC curve comparisons between suggested SVM-based approaches and cutting-edge rivals.

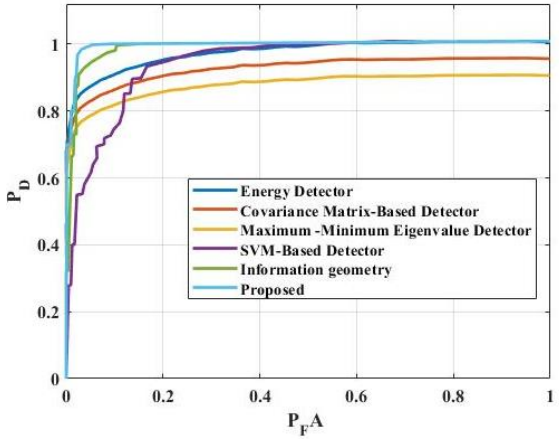

Fig. 7: Probability Distribution Comparison Analysis with Proposed Technique

Figure 7 illustrates the contrast between the SVM-based technique described in this study and the three existing detectors. The performance achieved is noteworthy as it surpasses that of covariance-based detectors and approaches that of the energy detector. It is important to note that this performance is achieved without the need for knowledge of the noise power. It should be mentioned that in order to estimate the noise power, training data was utilized, resulting in the threshold corresponding to the nominal probability of false alarm (P_{FA}). Figure 7 illustrates the contrast between extended and standard SVM-based approaches. The use of the noise power level in conjunction with the energy detector makes it a valuable tool. In general, support vector machine (SVM)-based detectors have the potential to achieve superior performance even in the absence of the aforementioned data, such as comparison plots of the simulated and measured results of the recommended wideband spectrum sensing receiver (WSSR) output, performance evaluations of the proposed minimum error distance (MED)-based spectrum sensing approach, or the graphical representation depicting the relationship between network utility and time.

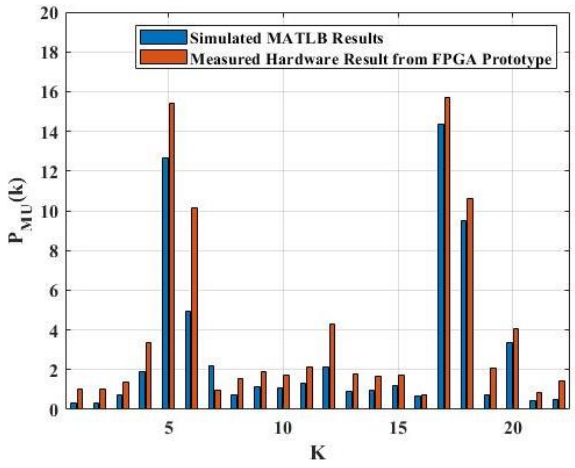

Fig. 8: Comparison Plots of Simulated and Measured Results

The output waveform has a distinct representation of the active channel configuration $\boldsymbol{PU_{MU}}(\widehat{\boldsymbol{k}})\ \forall\ \widehat{\boldsymbol{k}} = \{\mathbf{4},\mathbf{5},\mathbf{11},\mathbf{16},\mathbf{17}\}$ are stated to high value after $\prod$ = 2162 clock cycles. Additionally, we have conducted a comparison between the MATLAB generated values and the values obtained by FPGA measurements,$\boldsymbol{P_{MU}}\ (\boldsymbol{k})\ \forall\ \boldsymbol{k}\ =\ \{\mathbf{0},\mathbf{1},\mathbf{2},\cdots\ \boldsymbol{L}\ -\ \mathbf{1}\}$, as illustrated in figure 8.

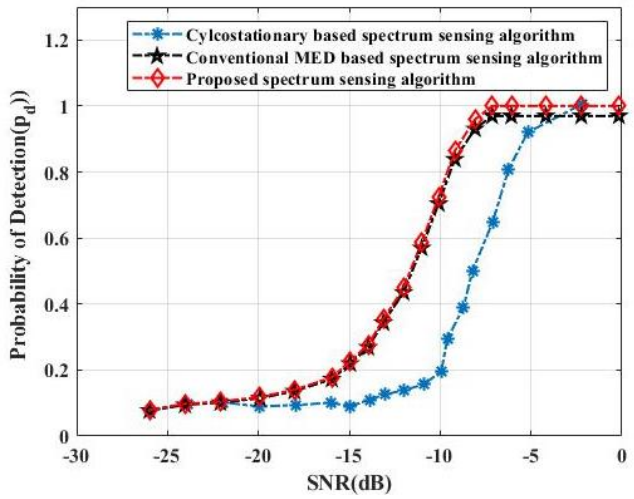

Fig. 9: SNR Performance Comparison of Proposed MED-Based Spectrum Sensing Algorithm

The use of the Monte-Carlo simulation technique has been authorized for the purpose of evaluating performance, as seen in Figure 8. The results indicate that the hardware-efficient MED-based spectrum sensor outperforms CSS by a margin of 4.5 dB at a probability of detection (P_d) of 0.5. Therefore, in the case of signals with strong correlation, the MED-based spectrum sensor demonstrates superior recital as related to both the energy uncovering founded spectrum sensor and CSS. Furthermore, it can be shown from Figure 9 that the hardware-efficient MED-based SSA exhibits a little decrease of 0.12 dB at a probability of detection (P_d) of 0.5 when compared to the traditional MED-based SSA.

6. Research Conclusion

The research investigated a hardware-effective spectrum sensor architecture for CRNs based on SMED. The principles of MED were utilised, along with the statistical properties of the received signal, to achieve hardware efficiency in the projected design. The projected architecture greatly reduced the hardware complexity and resource needs compared to conventional spectrum sensing approaches by making use of a simplified circuitry design. The proposed SMED-based spectrum sensor architecture's performance evaluation demonstrated its capacity to accurately classify the attendance of PUs in the spectrum. Its excellent detection accuracy and robustness even in the existence of noise, fading, and intrusion make the architecture suited for deployments of cognitive radio in the real world. In cognitive radio devices with incomplete capitals, power consumption is a crucial consideration. By reducing computational complexity and omitting pointless processing steps, the suggested design achieved impressive power efficiency. This power-saving capacity is essential for increasing the battery life of cognitive radio devices and making it possible for them to be used effectively in settings with limited energy resources.

The development of a hardware-efficient architecture with a fast sensing time for spectrum sensors based on the Minimum Euclidean Distance (MED) method was facilitated by using software provided by Xilinx. A real-world hardware test setup is used to validate the proposed Cooperative Spectrum Sensor (CSR)'s functionality, and an FPGA prototype of the CSR is also described here. Additionally, this CSR design has been ASIC synthesised in the UMC 90 nm-CMOS process through a 1.2 V supply and post-layout simulation has been performed on it. In the end, a real-world testing environment was used to test and verify the CSR-fabricated ASIC chip. The planned CSR is area-efficient and takes up less space (0.365mm2) than the traditional implementation, according to comparison results. The proposed architecture exhibited scalability and adaptability by accommodating different system configurations and varying signal environments. It handles a wide range of signal bandwidths and adapts to dynamic changes in spectrum availability, ensuring the spectrum sensing operation's flexibility and versatility. The proposed MED spectrum sensor has a reduced sensing time of less than 40 microseconds and achieves the lowest area-time-product among existing implementations, hence demonstrating superior hardware efficiency. The simulation findings demonstrate that the suggested detectors exhibit superior detection performance, especially when confronted with limited sample sizes, in comparison to other approaches.

References

[1] Chaurasiya, R.B. and Shrestha, R., 2019. Hardware-efficient and fast sensing-time maximum-minimum-eigenvalue-based spectrum sensor for cognitive radio network. IEEE Transactions on Circuits and Systems I: Regular Papers, 66(11), pp.4448-4461.

[2] Mukherjee, A., Li, M., Goswami, P., Yang, L., Garg, S. and Piran, M., 2021. Hybrid NN-based green cognitive radio sensor networks for next-generation IoT. Neural Computing and Applications, pp.1-9.

[3] Kumar, A., Khan, A.S., Modanwal, N. and Saha, S., 2020. Experimental studies on energy and eigenvalue based spectrum sensing algorithms using USRP devices in OFDM systems. Radio Science, 55(8), pp.1-11.

[4] Ciflikli, C. and Ilgin, F.Y., 2020. Studentized extreme eigenvalue based double threshold spectrum sensing under noise uncertainty. Tehnički vjesnik, 27(2), pp.353-357.

[5] Negi, B.S., Singh, O. and Khairnan, C., 2019. Enhancing Entropy Based Spectrum Sensing using

Eigen Value Decomposition in Cognitive Radio Networks. International Journal of Engineering Research and Technology, 12(7), pp.1008-1013.

[6] Chaurasiya, R.B. and Shrestha, R., 2019, May. Hardware-efficient and low sensing-time VLSI-architecture of MED based spectrum sensor for cognitive radio. In 2019 IEEE International Symposium on Circuits and Systems (ISCAS) (pp. 1-5). IEEE.

[7] Zheng, S., Chen, S., Qi, P., Zhou, H. and Yang, X., 2020. Spectrum sensing based on deep learning classification for cognitive radios. China Communications, 17(2), pp.138-148.

[8] Çiflikli, C. and Ilgin, F.Y., 2020. Multiple antenna spectrum sensing based on glr detector in cognitive radios. Wireless Personal Communications, 110(4), pp.1915-1927.

[9] Develi, I., 2020. Spectrum sensing in cognitive radio networks: threshold optimization and analysis. EURASIP Journal on Wireless Communications and Networking, 2020(1), pp.1-19.

[10] Khayyeri, M. and Mohammadi, K., 2020. Cooperative wideband spectrum sensing in cognitive radio based on sparse real-valued fast Fourier transform. IET Communications, 14(8), pp.1340-1348.

[11] Shen, Z. and Wang, Q., 2020. A High-Precision Spectrum-Detection Algorithm Based on the Normalized Variance of Nonreconstruction Compression Sensing. Mathematical Problems in Engineering, 2020.

[12] Varma, A.K. and Mitra, D., 2020. Cognitive Wideband Sensing Using Correlation Of Inverted Spectrum Segments. Revue Roumaine DES Sciences Techniques-Serie Electrotechnique Et Energetique, 65(1-2), pp.97-102.

[13] Goyal, S.B., Bedi, P., Kumar, J. and Varadarajan, V., 2021. Deep learning application for sensing available spectrum for cognitive radio: An ECRNN approach. Peer-to-Peer Networking and Applications, 14(5), pp.3235-3249.

[14] Fouda, H.S., Nasr, M.E. and Hussein, A.H., 2022. A highly efficient approach for performance enhancement of multiple antenna elements based spectrum sensing techniques using side lobe level reduction. Alexandria Engineering Journal, 61(8), pp.5983-5999.

[15] Mahendru, G., 2021. A novel double threshold-based spectrum sensing technique at low SNR under noise uncertainty for Cognitive Radio Systems.

[16] Giri, M.K. and Majumder, S., 2021. Eigenvalue-based cooperative spectrum sensing using kernel fuzzy c-means clustering. Digital Signal Processing, 111, p.102996.

[17] Du, L., Fu, Y., Chen, Y., Wang, X. and Zhang, X., 2021. Eigenvalue-Based Spectrum Sensing with Small Samples Using Circulant Matrix. Symmetry, 13(12), p.2330.

[18] Chaurasiya, R.B. and Shrestha, R., 2021, May. Hardware-efficient ASIC implementation of eigenvalue based spectrum sensor reconfigurable-architecture for cooperative cognitive-radio network.In 2021 IEEE International Symposium on Circuits and Systems (ISCAS) (pp. 1-5). IEEE.

[19] Liu, R., Ma, Y., Zhang, X. and Gao, Y., 2021. Deep learning-based spectrum sensing in space-air-ground integrated networks. Journal of Communications and Information Networks, 6(1), pp.82-90.

[20] Jie, Q., Zhan, X., Shu, F., Ding, Y., Shi, B., Li, Y. and Wang, J., 2022. High-performance Passive Eigen-model-based Detectors of Single Emitter Using Massive MIMO Receivers. IEEE Wireless Communications Letters.

[21] Al-Amidie, M., Al-Asadi, A., Humaidi, A.J., Al-Dujaili, A., Alzubaidi, L., Farhan, L., Fadhel, M.A., McGarvey, R.G. and Islam, N., 2021. Robust Spectrum Sensing Detector Based on MIMO Cognitive Radios with Non-Perfect Channel Gain. Electronics, 10(5), p.529.

[22] Nasser, A., Chaitou, M., Mansour, A., Yao, K.C. and Charara, H., 2021. A deep neural network model for hybrid spectrum sensing in cognitive radio. Wireless Personal Communications, 118(1), pp.281-299.

[23] Biswas, D.K. and Mahbub, I., 2021, January. A low-power duty-cycled impulse-radio ultrawideband (ir-uwb) transmitter with bandwidth and frequency reconfigurability scheme designed in 180 nm CMOS process. In 2021 IEEE Radio and Wireless Symposium (RWS) (pp. 49-52). IEEE.

[24] Aswatha, R., Dhivya, S., Priyadharsini, S., Soundararaj, R.D. and Nithya, S., Implementation of Eigenvalue Based Cooperative Spectrum Sensing in Cognitive Radio.

[25] Feng, Y., Xu, W., Zhang, Z. and Wang, F., 2022. Continuous Hidden Markov Model Based Spectrum Sensing with Estimated SNR for Cognitive UAV Networks. Sensors, 22(7), p.2620.

[26] Yaseen, M., Hayder Sabah Salih, Mohammad Aljanabi, Ahmed Hussein Ali, & Saad Abas Abed. (2023). Improving Process Efficiency in Iraqi universities: a proposed management information system. Iraqi Journal For Computer Science and Mathematics, 4(1), 211–219. https://doi.org/10.52866/ijcsm.2023.01.01.0020

[27] Aljanabi, M. ., & Sahar Yousif Mohammed. (2023). Metaverse: open possibilities. Iraqi Journal For Computer Science and Mathematics, 4(3), 79–86. https://doi.org/10.52866/ijcsm.2023.02.03.007

[28] Atheel Sabih Shaker, Omar F. Youssif, Mohammad Aljanabi, ABBOOD, Z., & Mahdi S. Mahdi. (2023). SEEK Mobility Adaptive Protocol Destination Seeker Media Access Control Protocol for Mobile WSNs. Iraqi Journal For Computer Science and Mathematics, 4(1), 130–145. https://doi.org/10.52866/ijcsm.2023.01.01.0011

[29] Hayder Sabah Salih, Mohanad Ghazi, & Aljanabi, M. . (2023). Implementing an Automated Inventory Management System for Small and Medium-sized Enterprises. Iraqi Journal For Computer Science and Mathematics, 4(2), 238–244. https://doi.org/10.52866/ijcsm.2023.02.02.021

[30] Gopalakrishnan Subburayalu, Hemanand Duraivelu, Arun Prasath Raveendran, Rajesh Arunachalam, Deepika Kongara & Chitra Thangavel (2023) Cluster Based Malicious Node Detection System for Mobile Ad-Hoc Network Using ANFIS Classifier, Journal of Applied Security Research, 18:3, 402-420, DOI: 10.1080/19361610.2021.2002118

[31] Maria Gonzalez, Machine Learning for Anomaly Detection in Network Security , Machine Learning Applications Conference Proceedings, Vol 1 2021.

[32] Kumar, C. ., & Muthumanickam, T. . (2023). Analysis of Unmanned Four-Wheeled Bot with AI Evaluation Feedback Linearization Method. International Journal on Recent and Innovation Trends in Computing and Communication, 11(2), 138–142. https://doi.org/10.17762/ijritcc.v11i2.6138